# Affinity Enhancement Bivalent Morpholino for Pretargeting: Initial Evidence by Surface Plasmon Resonance

Jiang He,* Guozheng Liu, Jean-luc Vanderheyden, Shuping Dou, Rusckoswki Mary, and Donald J. Hnatowich*

Division of Nuclear Medicine, Department of Radiology, University of Massachusetts Medical School, 55 Lake Avenue North, Worcester, Massachusetts 01655. Received November 22, 2004; Revised Manuscript Received January 31, 2005

Pretargeting with bivalent effectors capable of bridging antitumor antibodies has been reported to provide superior results by affinity enhancement. Morpholinos (MORFs) and other DNA analogues used for pretargeting are ideally suited as bivalent effectors since they are easily synthesized and the distance between binding regions, likely to be a determinant of binding, may be adjusted simply by lengthening the chain. The goal of this investigation was to synthesize a bivalent MORF and to determine by surface plasmon resonance (SPR) whether the bivalent MORF exhibited bimolecular binding and whether the MORFs showed improved in vitro hybridization affinity in its bivalent form compared to its monovalent form. An 18 mer amino-derivitized MORF was made bivalent by dimerizing with disuccinimidyl suberate (DSS) in 1-methyl-2-pyrrolidinone (NMP) with *N*,*N*-diisopropylethylamine (DIEA) followed by purification by ion exchange chromatography. The in vitro hybridization affinity of bivalent compared to monovalent MORF was then measured by SPR. For these measurements, the complementary biotinylated cDNA was immobilized at coating densities that provided an average spacing of 20−100 Å and used to investigate the influence of this spacing on binding of the bivalent MORF with its binding regions separated by 25 Å. The yield of bivalent MORF was as high as 45%, and the structure was confirmed by MALDI-TOF mass spectroscopy. When the sensograms obtained by SPR were analyzed using different binding models, the evidence was consistent with bimolecular binding of the bivalent MORF. The dissociation rate constant of the bivalent compared to monovalent MORF was more than 10-fold lower at 2.14 compared to $0.27 \times 10^{-5}$ (1/s) ($p < 0.05$), and since the association rate constants were similar at 8.53 and $5.64 \times 10^5$ (1/M·s) ($p = 0.08$), the equilibrium constant for hybridization to the immobilized cDNA of the bivalent compared to the monovalent MORF was almost 20-fold higher at 3.99 compared to $0.21 \times 10^{10}$ (1/M) ($p < 0.05$). In addition, qualitative evidence for bivalent binding of the bivalent MORF was apparent in the lower concentrations necessary to saturate the cDNA. Finally, the stoichiometry interpretation of the binding data provided estimates of the fraction of bivalent MORF binding bimolecularly. Under one set of conditions, this value was 20%. In conclusion, a bivalent MORF was easily synthesized by dimerization of a monovalent MORF. A lower dissociation rate constant and higher equilibrium constant was measured by SPR for the bivalent compared to monovalent MORF in their binding to an immobilized cDNA. These results show that bimolecular binding was occurring in the case of the bivalent MORF and suggest that bivalency may be superior to monovalency in MORF pretargeting applications.

## INTRODUCTION

While conventional immunoscintigraphy using monoclonal antibody promises to provide reliable noninvasive detection and localization of tumor, it still often provides marginal results in that image interpretation is often obscured by nonspecific accumulations of radioactivity in bone marrow, liver, in the vascular system, and other organs. As such, alternative methods with superior target/nontarget ratio are needed. Arguably one of the more attractive alternative approaches involves pretargeting (*1*). Preclinical studies of pretargeting have clearly demonstrated efficacy, and early clinical trials in several laboratories are providing encouraging results. These studies usually involve procedures based on the interaction of biotin with (strept)avidin, bispecific antibodies with a radiolabeled hapten, and oligonucleotides with their complement (*1*−*3*).

Even though (strept)avidin can be immunogenic, especially when conjugated to antibodies, and endogenous biotin can interfere, recent developments in avidin derivatives and biotin dimers or trimers are providing encouraging results (*4, 5*). However, the alternative approach using bifunctional antibodies as the first injectate and bivalent haptens (i.e. effector) as the second injectate has occasionally provided excellent results in animals with high tumor/normal tissue ratios and absolute tumor accumulations (*6*−*8*). These successes have been attributed in large part to affinity enhancement resulting from the bridging of two antibodies on the tumor surface by the radiolabeled bivalent hapten effector (i.e. "affinity enhancement system" or AES). The bivalent haptens used successfully include Ac-Lys(In-DTPA)-Tyr-Lys(In-DTPA)-Lys(TscG-Cys-)-$NH_2$ (*6, 9*), Janus bivalent hapten (*10*), pGlu-Leu-Tyr-Glu-Asn-Lys(DTPA)-Pro-Arg-Arg-Pro-Tyr-Ile-Leu and DTPA-Gly-

* To whom correspondence should be addressed. Phone: 508-856-2187 (J.H.); 508-856-4256 (D.J.H.); Fax: 508-856-4572 (J.H. and D.J.H.). E-mail: jiang.he@umassmed.edu; Donald.hnatowich@umassmed.edu.

10.1021/bc049719c CCC: $30.25 
Published on Web 03/01/2005

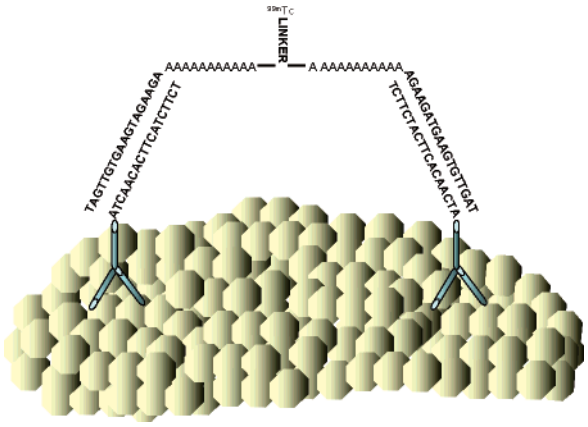


**Figure 1.** Artist's conception of a bivalent MORF bridging two complementary MORFs immobilizaed on a tumor cell.

Glu-Leu-Tyr-Glu-Asn-Lys(Ac)-Pro-Arg-Arg-Pro-Tyr-Ile-Leu (DTPA-Gly-NT) (*11*), and Ac-Phe-Lys(-DTPA)-Tyr-Lys(DTPA)-$NH_2$ (*12*) and have been variously radiolabled with $^{99m}$Tc, $^{188}$Re, $^{125}$I, $^{131}$I, $^{111}$In, and most recently $^{68}$Ga for radioimmunodetection and radiotherapy of tumor models (*13*−*21*). From these studies, it may be estimated that about 25 Å between the binding sites has been successfully used previously. Furthermore, a recent publication has shown that a bivalent receptor binding agent showed a 200-fold increase in affinity as the spacer between binding sites varied from 4 to 20 carbon atoms (i.e. 5−25 Å) (*22*).

This laboratory has previously reported encouraging results in tumored mice with pretargeting but using DNA and its analogues (collectively: oligomers). Instead of bifunctional antibodies, an antitumor antibody conjugated with a phosphodiamidate morpholine (MORF) serves as the first injection while the radiolabel is administered later on the complementary MORF (i.e. cMORF) as effector (*23*−*26*).

One advantage of using oligomers for pretargeting is the ease with which bivalent effectors for AES targeting may be constructed and the ease with which the molecular dimension separating the binding sites may be shortened or elongated. To accomplish the first goal of preparing the bivalent effector, MORFs with a primary amine were purchased and dimerized as described below. In future studies, the dimensions between binding sites will be investigated by purchasing the MORFs with additional bases in the chain.

The concept is shown schematically in Figure 1. In this investigation, we describe an initial test in which one bivalent MORF was synthesized and investigated for its properties of hybidization compared to its monovalent form. To measure these properties, a biotinylated cDNA was immobilized on a sensor chip at two concentrations, and, by surface plasmon resonance (SPR), the hybridization properties of MORF were measured in its bivalent form and compared to its monovalent form.

## MATERIALS AND METHODS

All 18 mer MORFs and cMORFs [collectively: (c)MORFs] whether biotinylated or amine modified on the 3′ equivalent end were purchased prepurified (Gene-Tools, Corvallis, OR) and were used as received. The MORF base sequence was 5′-equivalent-TCT-TCT-ACT-TCA-CAA-CTA-linker-primary amine. The linker for amine modification was $-C(O)OCH_2C_6H_4CH_2NH_2$. The base sequences of the cMORFs were complementary with the linker and primary amine also on the 3′ equivalent end. The molecular weights were 6164 and 6422 Da. Biotinylated (c)DNA having the same sequences as the (c)MORF were purchased from Qiagen Inc. (Valencia, CA) and were also used as received. Disuccinimidyl suberate (DSS) was purchased from Pierce (Rockford, IL). Anhydrous dimethylformamide (DMF), *N*-methyl-2-pyrrodinone (NMP), and diisopropylethylamine (DIEA) were purchased from Sigma-Aldrich (St. Louis, MO). All other chemicals were reagent grade and were used without purification.

**Preparation of Bivalent MORF.** About 1.5 mg (0.25 μmol) of amino-derivitized MORF was dissolved in 1.0 mL of 1-methyl-2-pyrrolidinone (NMP). A 0.125 μmol of disuccinimidyl suberate (DSS) in NMP solution at 2 mg/mL was added and followed by 0.66 μmol of *N*,*N*-diisopropylethylamine (DIEA). This mixture was incubated at room temperature for 2 days. The bivalent MORF was purified by Q Sepharose ion exchange chromatography. The collected fractions of bivalent MORFs were passed through a PD-10 column in 50 mM phosphate buffer. The molecular weight of the product was confirmed by MALDI-TOF before storage at freezer temperatures for future use.

**Chromatography.** Ion Exchange (IE) HPLC was performed on a HiTrap Q HP column (Amersham Biosciences, Uppsala Sweden) using 0.01 N NaOH (solvent A) and 0.01 N NaOH in 2 N NaCl (solvent B) at a flow rate of 1.0 mL/min going from 100% A to 70% A over the 30 min. Before each analysis, the column was stabilized with 0.01 N NaOH, and after each analysis the column was cleaned with solvent B. For small scale of preparative purification, samples were loaded on the column by several injections in running solvent A but without exceeding the column's maximum binding capability. The bivalent MORF was collected in fractions during the gradient elution.

**Surface Plasmon Resonance Measurements.** The surface plasmon resonance analysis (SPR) was performed on a BIAcore 2000 (BIAcore, Piscataway, NJ) instrument operating at room temperature. In these measurements DNAs rather than MORFs were immobilized because of earlier difficulties in immobilizing biotinylated (c)MORFs. Several 5−10 μL amounts of biotinylated(c)DNAs at 20 nM were each added to a separate new streptavidin−dextran-coated sensor chip (SA) at a flow rate of 20 μL/min until a response of about 100 (±10) or 500 (±30) response units (RU) was reached. The absence of mass transfer effects was confirmed by running separately one concentration of free MORFs at three different flow rates (10, 30, and 75 μL/min) and demonstrating identical response and curve shape for both concentrations. When the identical measurement was performed on a sensor chip to which DNA was added to a response of 750 RU, evidence of mass transfer effects was observed, and accordingly this chip was not used in subsequent studies. Solutions of free monovalent and bivalent MORF were prepared at eight concentrations from 0.0 to 500 nM in the same running buffer (10 mM HEPES, 150 mM NaCl, 3.4 mM $Na_2EDTA$, 0.005% P20, pH 7.4) and injected separately onto the active (cDNA) or control (DNA) surface. Dissociation was followed for 25 min or 4 h. The chip surface was regenerated by injection of 100 mM HCl. To correct for nonspecific binding and refractive index changes, the control responses were subtracted from those obtained from the active surface. A minor baseline drift resulting from a slow dissociation of the complex on the active and control surfaces was eliminated by also subtracting sensograms obtained following the injection of running buffer (*27*).

In the first series of experiments, samples of monovalent and bivalent MORFs were run at seven concentrations on both the 100 and 500 RU chips and with a dissociation time of only 25 min. In the second series of experiments, all seven concentrations were again run but with a dissociation time of 4 h to obtain more accurate values for the dissociation rate constants. To conserve instrument time, the longer analysis was performed only on the 100 RU chip. Each measurement was repeated four times, and, as mentioned above, each sample was run on both the cDNA and DNA chips at the same surface density so that results with the latter could be use to correct for bulk refractive index changes (*27*).

**Sensorgram Kinetic Analysis.** Sensorgram curves were evaluated using numerical intergration algorithms (BIAevaluation 3.0, BIAcore, Piscataway, NJ). The algorithm may be programmed for simple monomolecular 1:1 Langmuir interactions of a monvalent analyte or for a bivalent analyte binding monomolecularly (i.e. A+L→AL where A is the analyte, in this case MORF, and L is immobilized ligand, in this case cDNA) or binding bimolecularly (i.e. AA+L→AAL and AAL+ L→LAAL). In addition the algorithm may be programmed to analyze globally (i.e. all analyte concentrations considered together to provide one value for each of the two rate constants, association and dissociation) or locally (i.e. each analyte concentration considered separately to provide one value for each of the two rate constants for each analyte concentration). In addition, in the case of bimolecular binding, the bimolecular binding algorithm can provide one value for each of the two rate constants for the first and second binding. An added complication in the case of bivalent analyte binding is the possibility that the binding may be either monomolecular or bimolecular and thus cannot be accurately modeled. To emphasis this fact, the rate constants in this report for bivalent MORFs are referred to as "apparent". Finally, the program provides for each analysis a Chi2 ($\chi^2$) value which is a statistical measure of how closely the model fits the experimental data. In general, $\chi^2$ values lower than about 10 signify a good fit. In each of these investigations comparing monovalent to bivalent MORFs, the concentrations were adjusted to the same molarity of analyte and therefore the MORF molarity of the bivalent analyte was twice that of the monovalent analyte.

**Stoichiometry of Bivalent MORF Binding.** The BIAcore instrument measures the mass of molecules bound to the sensor surface. Thus, the stoichiometry of the surface molecular complex (i.e. the number of analyte molecules per ligand molecule) can be determined using eq 1:

$$\text{stoichiometry} = (R_{A(max)} \times MW_L)/(MW_A \times R_L) \quad (1)$$

where MW refers to molecular weight of the analyte ($MW_A$) and immobilized ligand ($MW_L$) while $R$ refers to the response in RU of the analyte ($R_A$) and the ligand ($R_L$). $R_{A(max)}$ refers to the maximum response (i.e. binding capacity) of $R_A$ for any ligand concentration $R_L$ (i.e. either 100 or 500 RU) and can be obtained by analyzing locally the sensograms obtained at different analyte concentrations (*4, 28, 29*). If the stoichiometry value provided by eq 1 for monovalent MORF is fixed at 1.00, pure bimolecular binding of the bivalent MORF must provide a stoichiometry value of 0.50. To eliminate uncertainties related to ligand concentration in this investigation, the monovalent and bivalent MORFs were compared on the same sensor chips (and thus at the same $MW_L$ and $R_L$) and the stoichimetry of the bivalent MORF is expressed as a ratio of that of the bivalent over the monovalent MORF.

## RESULTS

**Preparation of Bivalent MORF.** To prepare the bivalent MORF, the amine derivatized MORF was dimerizing with disuccinimidyl suberate (DSS) for 2 days in the presence of 1-methyl-2-pyrrolidinone (NMP) and *N*,*N*-diisopropylethylamine (DIEA). The IE HPLC UV profile for the reaction mixture is shown in Figure 2C with peaks at 10.8, 11.8, and 13.9 min that are thought to represent the excess native MORF (shown in Figure 2A), DSS modified but monovalent MORF and the desired bivalent MORF, respectively. To help confirm these identifies, MORF was also reacted with succinic anhydride to give a compound similar to the DSS modified but monovalent MORF especially in the negative charge (Figure 2B). In this way, the remaining peak at 13.9 min was identified as the bivalent MORF (Figure 2D). Changing from alkaline solution to phosphate buffer or water was performed on a PD-10 column. Correct structure of the bivalent MORF was confirmed by MALDI-TOF MS (calculated MW: 12466; found: 12474 ± 8).

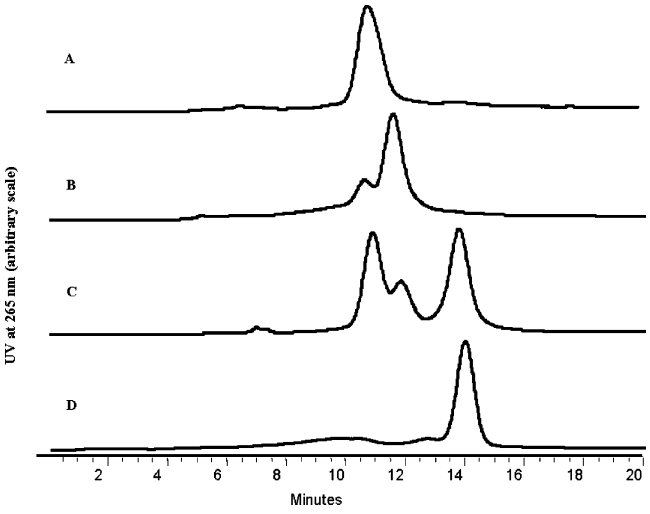


**Figure 2.** Chromatograms of native MORF (panel A), derivatized but monovalent MORF (panel B), the reaction mixture (panel C), and purified bivalent MORF (panel D) obtained by IE HPLC with UV detection.

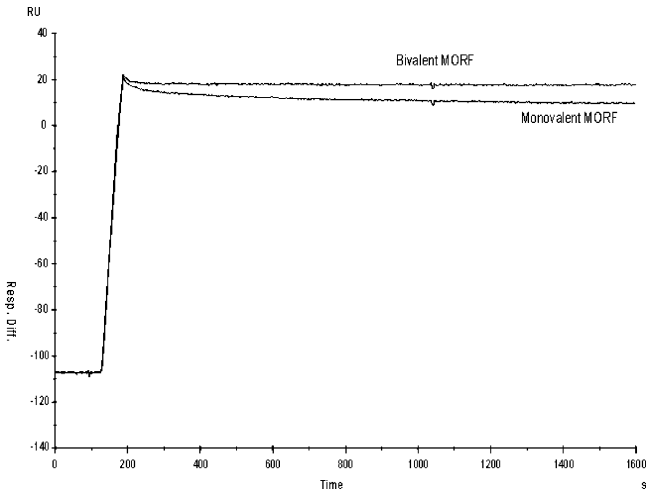


**Figure 3.** Typical sensograms (normalized) of monovalent and bivalent MORF and obtained at one concentration (40 nM) and at one cDNA density (100 RU).

**Table 1. Comparison of Apparent Kinetics Rate Constants and Equilibrium Constants for the Interaction of Monovalent and Bivalent MORF with Immobilized cDNA by Global Fitting Using the 1:1 Langmuir Interaction Model[a]**

| | | | $k_d$ (1/s) × $10^{-5}$ | | | | |
|---|---|---|---|---|---|---|---|
| cDNA density | analyte | $k_a$ (1/M·s) × $10^5$ | $k_d$ | $k_d$ fast | $k_d$ slow | $K_{equ}$ (1/M·s) × $10^{10}$ | $\chi 2$ |
| 100 RU | bivalent MORF | 8.52(1.32) | 2.14(0.39) | 26.3(4.7) | 0.22(0.04) | 3.99(0.83) | 17(8) |
| | monovalent MORF | 5.64(0.65) | 26.7(1.92) | 37.5(6.2) | 0.72(0.06) | 0.21(0.07) | 8(4) |
| 500 RU | bivalent MORF | 6.31(0.75) | 5.63(0.93) | 20.6(5.3) | 0.14(0.03) | 1.12(0.21) | 42(20) |
| | monovalent MORF | 5.12(0.71) | 29.3(1.24) | 33.1(9.4) | 0.68(0.05) | 0.18(0.48) | 12(7) |

[a] $k_a$: association rate constant; $k_d$: dissociation rate constant; $K_{equ}$: equilibrium constant; $\chi^2$: index for goodness of fit. Standard deviations in parentheses.

**Table 2. Comparison of Equilibrium Constants for the Binding of Monovalent MORF and Bivalent MORF to Immobilized cDNA by Local Fitting Using the 1:1 Langmuir Interaction Model[a]**

| concentration (nM) | | 400 | 250 | 160 | 80 | 40 | 20 | 10 |
|---|---|---|---|---|---|---|---|---|
| 500 RU, bivalent MORF | $K_{equ}$((1/M·s) × $10^9$) | 17.4 | 6.76 | 4.94 | 4.23 | 3.23 | 1.75 | 2.31 |
| | $\chi^2$ | 6.23 | 7.77 | 3.56 | 5.21 | 1.32 | 0.23 | 4.02 |
| 500 RU, monovalent MORF | $K_{equ}$((1/M·s) × $10^9$) | 2.74 | 2.13 | 1.34 | 3.65 | 4.23 | 2.39 | 2.45 |
| | $\chi^2$ | 1.35 | 6.53 | 5.66 | 4.32 | 2.65 | 2.79 | 4.36 |
| 100 RU, bivalent MORF | $K_{equ}$((1/M·s) × $10^9$) | 1.00 | 2.23 | 19.9 | 18.7 | 2.22 | 1.42 | 9.69 |
| | $\chi^2$ | 1.85 | 2.64 | 0.76 | 1.93 | 0.55 | 0.72 | 16 |
| 100 RU, monovalent MORF | $K_{equ}$((1/M·s) × $10^9$) | 3.69 | 3.42 | 2.16 | 1.97 | 2.75 | 3.20 | 1.26 |
| | $\chi^2$ | 0.63 | 1.12 | 0.98 | 3.12 | 0.71 | 2.65 | 1.63 |

[a] $K_{equ}$: equilibrium constant; $\chi^2$: index for goodness of fit.

**Table 3. Comparison of Apparent Kinetic Rate Constants for the Binding of Bivalent MORF with cDNA Immobilized at 100 RU by Using the Bivalent Binding Model and Local Fitting**

| concentration of bivalent MORF (nM) | 400 | 250 | 160 | 80 | 40 | 20 | 10 |
|---|---|---|---|---|---|---|---|
| $k_a(1 \times 10^5)$ (1/M·s) | 4.74 | 1.03 | 7.25 | 6.89 | 3.99 | 2.18 | 9.92 |
| $k_d(1 \times 10^{-4})$ (1/s) | 20.3 | 9.07 | 31.4 | 35.1 | 30.3 | 3.39 | 2.59 |
| $k_a(2 \times 10^{-3})$ (1/M·s) | 9.40 | 1.30 | 4.30 | 2.30 | 0.20 | 0.80 | 4.36 |
| $k_d(2 \times 10^{-5})$ (1/s) | 21.7 | 6.68 | 5.02 | 2.41 | 1.39 | 3.52 | 1.72 |
| $\chi^2$ | 0.677 | 4.99 | 0.545 | 1.01 | 1.89 | 15.3 | 0.65 |

**Sensorgram Kinetic Analysis.** Figure 3 is a composite presenting typical sensorgrams for the monovalent and the bivalent MORFs obtained at 40 nM concentration with cDNA immobilized at 100 RU. The figure shows that the dissociation of bivalent MORF is slower compared to monovalent MORF and almost imperceptible over the 23 min dissociation period, a result of its high binding affinity. To measure more accurately the dissociation rate constant, the binding studies were repeated with a 4 h dissociation period. The measurement was performed for both surface densities of 100 and 500 RU and at seven concentrations of the monovalent and bivalent MORF from 0.5 to 500 nM. The results for different models and fitting method (globally or locally) are reported in Tables 1−3. Table 1 presents a comparison of the results obtained in the analysis of sensograms obtained with the monovalent and bivalent by the simpler 1:1 Langmuir interaction algorithm with global fitting. Table 2 presents analysis of the same data by the 1:1 Langmuir interaction algorithm but with local fitting. Finally Table 3 presents an analysis of only those sensograms obtained with the bivalent MORF using local fitting but with the bivalent algorithm rather than 1:1 Langmuir interaction algorithm. In each case, the $\chi^2$ value is included as a statistical measure of how closely the model fits the experimental data.

As shown in the table, by globally fitting using a 1:1 Langmuir interaction algorithm, the association rate constants are similar for both monovalent and bivalent MORF. However, there is a significant difference in dissociation rate constants providing an equilibrium constants 15−20 times higher for the bivalent MORF at both cDNA densities.

A key step in interpreting the BIAcore results may be the separation of the dissociation rate constants into fast and slow phases since that may provide a method of distinguishing bimolecular binding of the bivalent MORF from monomolecular binding (*30, 31*). In the case of bivalent MORF, monomolecular binding should provide the same dissociation behavior as monovalent MORF while bimolecular binding should show different and slower dissociation kinetics. As described below, by inspection of the dissociation curves, the fast phase was defined as completed by 2 min following the end of the injection while the slow phase continued thereafter. The results are presented in Table 1 as $k_d$ of fast and slow phases.

As shown in Table 2, a more complicated analysis again using the 1:1 Langmuir interaction algorithm but with local fitting has provided a better fit with more reasonable $\chi^2$ usually less than 8. As shown, for the bivalent MORF the highest affinity at the 100 RU density was found in the concentration range of 80−160 nM while at density of 500 RU the highest affinity started at 250 nM.

Table 3 presents the apparent kinetics rate constants of bivalent MORF at different concentrations under condition of 100 RU DNA density and using the bivalent binding model instead of the 1:1 Langmuir interaction algorithm. The bivalent model considers the association and dissociation of the first and second bindings separately. Using a bivalent model to locally fit the sensorgrams of bivalent MORF has generally produced even lower $\chi^2$ values and therefore a superior fit.

Figure 4 A and B presents sensograms of the monovalent and bivalent MORFs at different concentrations and at one cDNA density. Interpretation of the senso-

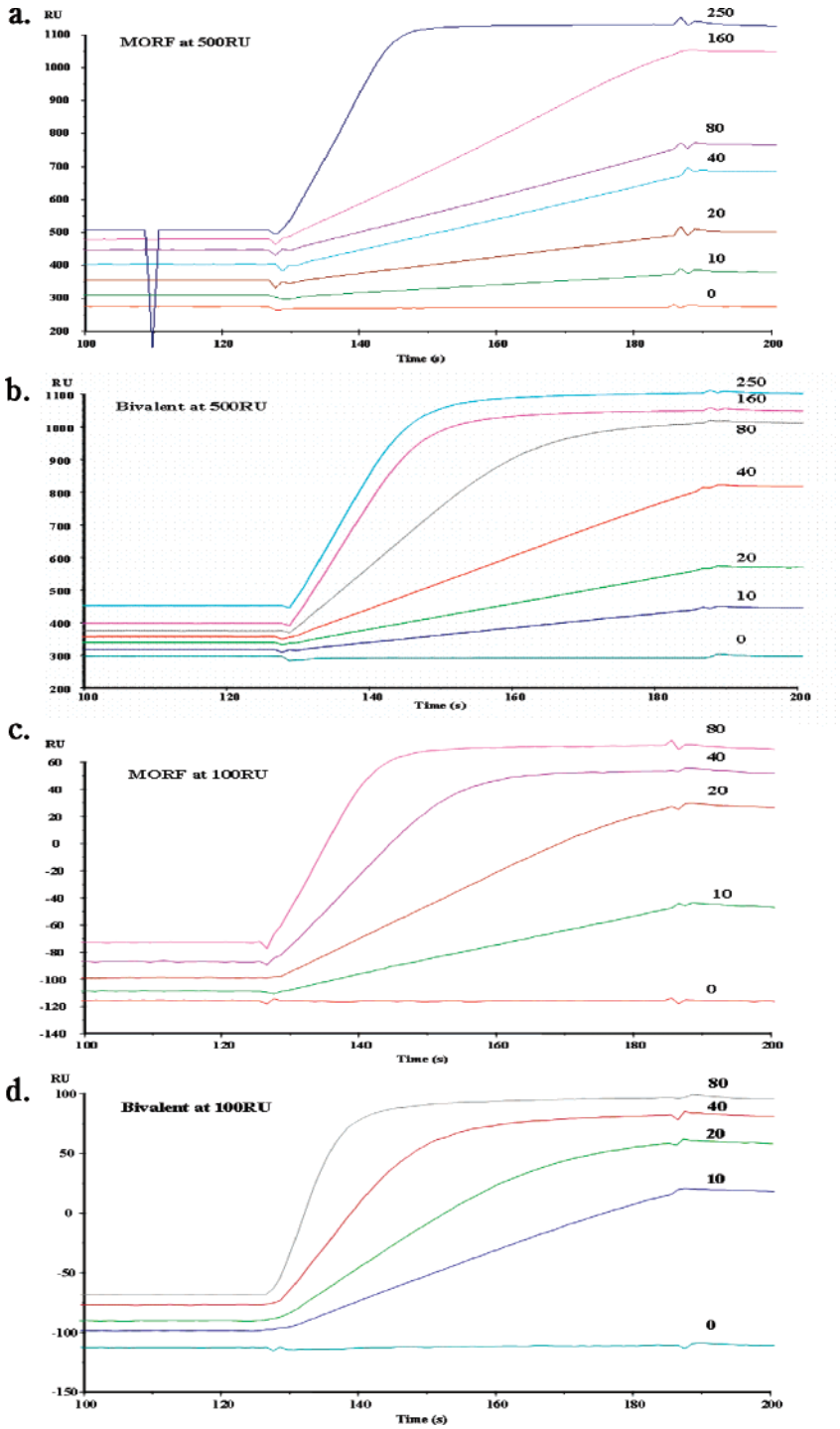


**Figure 4.** Sensograms at 500 RU cDNA density of the monovalent (panel A) and bivalent MORF (panel B) and at 100 RU cDNA density of the monovalent (panel C) and bivalent MORF (panel D) at the concentrations shown. The MORF concentrations of the bivalent MORF are twice the analyte concentrations. Concentraions are all in nM.

grams involves inspection of the behavior during injection (125 to 185 s). In the absence of saturation, the response will increase linearly throughout the entire period of the injection. In the presence of saturation, the response will level off before the end of the injection. Examples of both may be found in the sensograms of the bivalent MORF (Figure 4B). When injected at concentrations of 40 nM or less, the response increases linearly throughout while at higher concentration, the response becomes horizontal before the end of the injection and does so earlier with increasing concentration. The monovalent MORF clearly reaches a steady response more rapidly than bivalent MORF at this cDNA density and also does so at the lower cDNA density (Figure 4C and 4D). The sensograms may also be inspected for the shape of the curves as saturation approaches. In the case of the monovalent MORF, incapable of bimolecular binding, the sensograms shows a relatively abrupt change from increasing to horizontal response (Figure 4A and 4C). By contrast, the bivalent MORF shows a slower transition as evidence that more complex binding is occurring probably involving both monomolecular and bimolecular binding.

**Stoichiometry of Bivalent MORF with Immobilized cDNA.** The results of applying eq 1 to the sensograms showed that at both cDNA densities, the ratio of stoichiometry values for the bivalent over the monovalent

MORF is approximately 0.85 at all concentrations. Since this value is between the 1.0 for pure monomolecular binding and 0.5 for pure bimolecular binding, these results imply that the bivalent MORF under all conditions exhibits a mixture of monomolecular and bimolecular binding.

## DISCUSSION

In this investigation, SPR was used to study the behavior of a bivalent MORF compared to its monovalent form during hybridization to immobilized cDNA. The bivalent MORF, AA, may bind to one cDNA ligand, L, to form the complex AAL, or it may bridge two ligands to form the complex LAAL. The probability of monomolecular binding (AAL) compared to bimolecular binding (LAAL) will depend on the molecular dimensions of the bivalent analyte and the concentration (spacing) and flexibility of the ligand molecules on the immobilized surface (*32*). Since bimolecular binding may be expected to provide higher hybridization affinities (equilibrium constants) than monomolecular binding, bimolecular binding of bivalent analytes may be expected to be favored under favorable conditions.

By inspection of the sensograms, it is possible to conclude that bimolecular binding of the bivalent MORF was observed in this investigation. The slower dissociation kinetics of the bivalent compared to the monovalent MORF (Figure 3) may be best explained by bimolecular binding of the bivalent MORF leading to slower dissociation. Additional evidence is provided by examination of the dissociation rate in Table 1. As is evident from the Table, the dissociation rate is largely independent of cDNA density in the case of the monovalent MORF but shows a strong dependence on the cDNA density in the case of the bivalent MORF. At the lower cDNA density, monomolecular binding of the bivalent MORF is favored as a result of the larger spacing between cDNAs. The fraction of the bivalent MORF binding bimolecularly may be expected to increase with increasing cDNA density (and therefore decreasing spacing), and therefore the dissociation rate will decrease as shown.

Finally, the sensograms may be inspected for the shape of the association/dissociation phase during injection. At the higher 500 RU cDNA density, saturation (evident by a horizontal response before the end of the injection) required concentrations greater than 40 nM for the bivalent MORF while saturation was not achieved for the monovalent MORF at less than 160 nM. Even considering that the MORF concentration of the bivalent MORF is half that of the monovalent MORF at the same analyte concentration, it is apparent that higher concentrations are required to achieve saturation in the case of the monovalent MORF presumably because the bivalent MORF is capable of bridging cMORFs by bimolecular binding.

Evidence of bimolecular binding is also apparent in the results of applying eq 1 to estimate the stoichometry of binding. Since the response by SPR increases linearly with the molecular weight of the analyte, it should be possible to distinguish between monomolecular and bimolecular binding in the case of the bivalent MORF. Monomolecular binding of the bivalent MORF will provide a response related to its molecular weight that is double that of bimolecular binding for the same number of cDNAs bound. But in the case of bimolecular binding, the response between monovalent and bivalent MORF for the same number of cDNAs will be lower as bivalent MORF bridges two binding sites. This analysis is based on the assumption that the larger bivalent MORF shows no steric hindrance to cDNA binding monomolecularlly compared to the smaller monovalent MORF. There is therefore a different response at the same number of cDNA binding sites for pure bimolecular binding and pure monomolecular binding in the case of bivalent MORF that can be used to estimate the fraction of bivalent MORF that is binding bivalently. To correct for variations in cDNA density and MORF concentrations, the results of stoichiometry analysis have been presented as a ratio. Thus, pure monomolecular binding would results in a stoichiometry value of 1.00 while pure bimolecular binding would results in a value of 0.50. That the results are fairly constant at about 0.79−0.93 regardless of cDNA density or MORF concentration indicates that a substantial and fairly constant fraction of the bivalent binding is bimolecular under all conditions. A value of 0.8 corresponding to the binding of about four bivalent MORF to five cDNAs or only one of four bivalent MORF binding bimolecularily or 25%. In this manner it may be estimated that less than 20% of bivalent MORF was binding bimolecular under the conditions in this study.

Evidence for bimolecular binding may also be apparent from sensorgram analysis using numerical intergration algorithms (BIAevaluation 3.0, BIAcore, Piscataway, NJ). In this investigation, the dissociation curves were analyzed by separately considering a fast and a slow dissociation phase. Dissociation of the bivalent MORF will involve both the dissociation of monomolecular bound bivalent MORF similar to that of the monovalent MORF and the dissociation of biomolecularily bound MORF unique to the bivalent MORF (*30, 31*). In case of the bivalent MORF, monomolecular binding should therefore provide the same dissociation behavior as monovalent MORF while bimolecular binding should show different and slower dissociation kinetics. In this study, the fast phase was defined as completed by 2 min following the end of injection while the slow phase continued thereafter. The $k_d$ values for both phases are reported separately in Table 1 for both monovalent and bivalent MORF. In general, low cDNA density and higher MORF concentrations will not favor bimolecular binding, in the first instance because of the greater spacing between cDNAs and in the latter instance because the cDNAs are more likely to be saturated with MORF bound monomolecularly (see below). As evident in the table, at both cDNA densities, the $k_d$ fast values are similar for monovalent and bivalent MORF (indicating monomolecular binding) while the $k_d$ slow values for the bivalent MORF are significantly smaller ($p = 0.03$) at both densities (indicative of bimolecular binding). Thus, these results suggest that the bivalent MORF is binding bimolecularally at least in part.

The evidence presented above confirms that bimolecular binding was observed. It is then possible to examine the influence of bimolecular binding on the rate and equilibrium constants of hybridization. Bimolecular binding would be expected to result in lower dissociation rate constants and higher equilibrium constants. The results of analyzing the sensograms obtained in this investigation confirm that this is the case. As shown in Table 1, by globally fitting using a 1:1 Langmuir interaction algorithm, an important differences in dissociation rate constants is apparent between monovalent and bivalent MORF providing an equilibrium constant about 15−20 times higher for the bivalent MORF. Reanalysis using local fitting provided separate equilibrium constants for each MORF concentration. As shown in Table 2, in the

case of 500 RU cDNA density, the equilibrium constants for monovalent and bivalent MORFs are similar at concentrations below about 160 nM while at higher concentrations, the equilibrium constant for the bivalent MORF is approximately 2−8 times higher. The results of reanalyzing the data obtained at 100 RU cDNA density also shows similar equilibrium values at concentrations of 80 nM or less and about 9 times higher values for the bivalent MORF at concentrations of 80 and 160 nM. For reasons not understood, the trend reverses at higher concentrations with the monovalent MORF exhibiting higher equilibrium constants than the bivalent. Thus higher equilibrium constants and therefore affinity enhancement only occurred over a particular range of analyte concentrations in our bivalent MORF system instead of at all low concentrations as in other multivalent systems (*30*−*34*). This observation may be due to conformation changes during association of both the long, linear, and flexible cDNA linear ligands and MORF analytes and the complexity of oligomer hybridization itself involving many base pairs.

Table 3 presents the results of reanalyzing the results obtained for the bivalent MORF at each concentration but only at the 100 RU cDNA density. This analysis was capable of calculating separately an apparent first and second association and dissociation rate constants. As shown in the table, the apparent first association rate constant for all concentrations are similar ($(1-7) \times 10^5$ 1/M·s), indicating similar behavior in the first binding step regardless of concentration as is reasonable for consistent monomolecular binding. Furthermore, the first association rate constant is much larger (i.e. more rapid first association) compared to second association rate constant as is reasonable since bimolecular binding requires reorientation. Therefore, high concentrations of bivalent MORF will tend to saturate cDNA sites with monomolecular binding first, reducing the chances for bimolecular binding and therefore reducing the equilibrium constant. This phenomenon may be expected to be more pronounced at lower cDNA concentrations.

It is important to point out that in the sensogram analysis, quantitative evaluation was made difficult by the high cDNA densities required in this investigation to achieve bimolecular binding. These high densities can result in mass transport effects and, furthermore, can complicate the analysis by permitting rebinding during dissociation. In this investigation it was possible to prevent mass transport complications by adjusting the flow rate to be in a range where the response was shown to be flow-rate-independent. However, it was not possible to eliminate rebinding effects, and thus rebinding contributed partially to the resulting kinetic analysis. However, as rebinding would be hindered under conditions of ligand saturation, the fact that bivalent MORF saturated the cDNA at much lower concentrations than monvalent MORF would imply more favorable affinity of bivalent MORF than estimated in this study.

In this investigation, affinity enhancement was observed for the bivalent MORF on chips with cDNA densities as low as 100 RU. The RU unit can be approximately converted to mass of protein in the dextran layer by the relation 1 RU = 1 pg/mm$^2$ (*35*). With a new SA chip at 10000 RU in strepavidin, there are 10000 pg SA/mm$^2$ or $1.66 \times 10^{-13}$ mol SA/mm$^2$. Using an 18 mer biotin-cDNA (MW ∼ 6K) as the ligand and assuming binding to all four sites of strepavidin, the maximun binding capacity of biotinylated cDNA may be estimated as 4.11 ng cDNA/mm$^2$ or $6.64 \times 10^{-13}$ mol cDNA/mm$^2$ which corresponds to 4000 RU of cDNA. Initially in this study, 100 RU, 500 RU, and 750 RU of cDNA were immobilized which correspond to a 82, 25, and 17 Å distance between two neighboring cDNA. However, at a practical coating density of 750 RU, the effects of mass transport limitation were evident (data not shown), and for this reason only the 100 RU and 500 RU coating densities were used for further studies. It may be surprising that the 82 Å average spacing between cDNAs at 100 RU density did allow bimolecular binding for the bivalent MORF with about 25 Å between two MORF. This could be explained both by the relatively long 17-atom linker by which the cDNA is tethered to the chip via the biotin group and that the MORF itself is about 61 Å long. The bivalent MORF may be expected to have a large access range.

## CONCLUSION

A synthesis of bivalent MORF has been described. The bivalent MORF exhibited significant enhanced affinity compared to monovalent MORF as demonstrated by BIAcore measurements. These results suggest that bivalency may be superior to monovalency in MORF pretargeting applications. Studies using less flexible ligand immobilization, lower coating density, and bivalent MORF with different length of linker will be necessary to optimize the influence of affinity enhancement of bivalent MORFs in pretargeting applications.

## ACKNOWLEDGMENT

Financial support for this investigation was provided, in part, by the National Institutes of Health (CA79507 and CA 94994). The authors are grateful to Dr. Yongfu Li of Gene-Tools, Inc. (Corvallis, OR) for advice on the MORF purification.

## LITERATURE CITED

(1) Goodwin, D. A., Meares, C. F., McTigue, M., Mccall, M. J., and David, G. S. (1986). Rapid localization of haptens in sites containing previously administered antibody for immunoscintigraphy with short half-life tracers [abstract]. *J. Nucl. Med. 27*, 959−959.

(2) Hnatowich, D. J., Virzi, F., and Rusckowski, M. (1987) Investigations of avidin and biotin for imaging applications. *J. Nucl. Med. 28*, 1294−302.

(3) Kuijpers, W. H., Bos, E. S., Kaspersen, F. M., Veeneman, G. H. and van Boeckel, C. A. (1993) Specific recognition of antibody-oligonucleotide conjugates by radiolabeled antisense nucleotides: a novel approach for two-step radioimmunotherapy of cancer. *Bioconjugate Chem. 4*, 94−102.

(4) Hamblett, K. J., Kegley, B. B., Hamlin, D. K., Chyan, M. K., Hyre, D. E., Press, O. W., Wilbur, D. S., and Stayton, P. S. (2002) A streptavidin−biotin binding system that minimizes blocking by endogenous biotin. *Bioconjugate Chem. 13*, 588−598.

(5) Wilbur, D., Pathare, P. M., Hamlin, D. K., and Weerawarna, S. A. (1997) Biotin Reagents for Antibody Pretargeting. 2. Synthesis and in Vitro Evaluation of Biotin Dimers and Trimers for Cross-Linking of Streptavidin. *Bioconjugate Chem. 8*, 819−832.

(6) Karacay H., McBride W. J., Griffiths G. L., Sharkey R. M., Barbet J., Hansen, H. J., and Goldenberg, D. M. (2000) Experimental pretargeting studies of cancer with a humanized anti-CEA x murine anti-[In-DTPA] bispecific antibody construct and a 99mTc-/188Re-labeled peptide. *Bioconjugate Chem. 11*, 842−854

(7) Gruaz-Guyon, A., Janevik-Ivanovska, E., Raguin, O., De Labriolle-Vaylet, C., and Barbet, J. (2001) Radiolabeled bivalent haptens for tumor immunodetection and radioimmunotherapy. *Q. J. Nucl. Med. 45*, 201−6.

(8) Chang, C., Sharkey, R. M., Rossi, E. A., Karacay, H., McBride, W., Hansen, H. J., Chatal, J., Barbet, J., and

Goldenberg, D. M. (2002) Molecular advances in pretargeting radioimmunotherapy with bispecific antibodies. *Mol. Cancer Ther. 1*, 553−563.

(9) Cardillo, T. M., Karacay, H., Goldenberg, D. M., Yeldell, D., Chang, C. H., Modrak, D. E., Sharkey, R. M., and Gold, D. V. (2004) Improved targeting of pancreatic cancer: experimental studies of a new bispecific antibody, pretargeting enhancement system for immunoscintigraphy. *Clin. Cancer Res. 10*, 3552−3561.

(10) Goodwin, D. A., Meares, C. F., McTigue, M., Chaovapong, W., Diamanti, C. I., Ransone, C. H., and McCall, M. J. (1992) Pretargeted immunoscintigraphy: Effect of hapten valency on murine tumor uptake. *J. Nucl. Med. 33*, 2006−2013.

(11) Hillairet De Boisferon, M., Raguin, O., Thiercelin, C., Dussaillant, M., Rostene, W., Barbet, J., Pelegrin, A., and Gruaz-Guyon, A. (2002) Improved tumor selectivity of radiolabeled peptides by receptor and antigen dual targeting in the neurotensin receptor model. *Bioconjugate Chem. 13*, 654−662.

(12) Boerman, O. C., van Eerd, J., Oyen, W. J. G., and Corstens, F. H. M. (2002) A 3-Step Pretargeting Strategy to Image Infection. *J. Nucl. Med. 42*, 1405−1411.

(13) Barbet, J., Peltier, P., Bardet, S., Vuillez, J. P., Bachelot, I., Denet, S., Olivier, P., Leccia, F., Corcuff, B., Huglo, D., Proye, C., Rouvier, E., Meyer, P., and Chatal, J. F. (1998) Radioimmunodetection of medullary thyroid carcinoma using indium-111 bivalent hapten and anti-CEA x anti-DTPA-indium bispecific antibody. *J. Nucl. Med. 39*, 1172−1178.

(14) Bardies, M., Bardet, S., Faivre-Chauvet, A., Peltier, P., Douillard, J. Y., Mahe, M., Fiche, M., Lisbona, A., Giacalone, F., Meyer, P., Gautherot, E., Rouvier, E.; Barbet, J., and Chatal, J. F. (1996) Bispecific antibody and iodine-131-labeled bivalent hapten dosimetry in patients with medullary thyroid or small-cell lung cancer. *J. Nucl. Med. 37*, 1853−1859.

(15) Gautherot, E., Rouvier, E., Daniel, L., Loucif, E., Bouhou, J., Manetti, C., Martin, M., Le Doussal, J. M., and Barbet, J. (2000) Pretargeted radioimmunotherapy of human colorectal xenografts with bispecific antibody and 131I-labeled bivalent hapten. *J. Nucl. Med. 41*, 480−487.

(16) Gestin, J. F., Loussouarn, A., Bardies, M., Gautherot, E., Gruaz-Guyon, A., Sai-Maurel, C., Barbet, J., Curtet, C., Chatal, J. F., and Faivre-Chauvet, A. (2001) Two-step targeting of xenografted colon carcinoma using a bispecific antibody and 188Re-labeled bivalent hapten: biodistribution and dosimetry studies. *J. Nucl. Med. 42*, 146−153.

(17) Griffiths, G. L., Chang, C. H., McBride, W. J., Rossi, E. A., Sheerin, A., Tejada, G. R., Karacay, H., Sharkey, R. M., Horak, I. D., Hansen, H. J., and Goldenberg, D. M. (2004) Reagents and methods for PET using bispecific antibody pretargeting and 68Ga-radiolabeled bivalent hapten-peptide-chelate conjugates. *J. Nucl. Med. 45*, 30−39.

(18) Hosono, M., Hosono, M. N., Kraeber-Bodere, F., Devys, A., Thedrez, P., Fiche, M., Gautherot, E., Barbet, J., and Chatal, J. F. (1998) Biodistribution and dosimolecular study in medullary thyroid cancer xenograft using bispecific antibody and iodine-125-labeled bivalent hapten. *J. Nucl. Med. 39*, 1608−1613.

(19) Hosono, M., Hosono, M. N., Kraeber-Bodere, F., Devys, A., Thedrez, P., Faivre-Chauvet, A., Gautherot, E., Barbet, J., and Chatal, J. F. (1999) Two-step targeting and dosimetry for small cell lung cancer xenograft with anti-NCAM/antihistamine bispecific antibody and radioiodinated bivalent hapten. *J. Nucl. Med. 40*, 1216−1221.

(20) Kraeber-Bodere, F., Bardet, S., Hoefnagel, C. A., Vieira, M. R., Vuillez, J. P., Murat, A., Ferreira, T. C., Bardies, M., Ferrer, L., Resche, I., Gautherot, E., Rouvier, E., Barbet, J., and Chatal, J. F. (1999) Radioimmunotherapy in medullary thyroid cancer using bispecific antibody and iodine 131-labeled bivalent hapten: preliminary results of a phase I/II clinical trial. *Clin. Cancer Res. 5(Suppl.)*, 3190s−3198s.

(21) Kraeber-Bodere, F., Faivre-Chauvet, A., Sai-Maurel, C., Campion, L., Fiche, M., Gautherot, E., Le Boterff, J., Barbet, J., Chatal, J. F., and Thedrez, P. (1999) Toxicity and efficacy of radioimmunotherapy in carcinoembryonic antigen-producing medullary thyroid cancer xenograft: comparison of iodine 131-labeled F(ab′)2 and pretargeted bivalent hapten and evaluation of repeated injections. *Clin Cancer Res. 5(10 Suppl)*, 3183s−3189s.

(22) Sridhar, J., Wei, Z., Nowak, I., Lewin, N. E., Ayers, J. A., Pearce, L. V., Blumberg, P. M., and Kozilowski, A. P. (2003) New bivalent PKC ligands linked by a carbon spacer: Enhancement in binding affinity. *J. Med. Chem. 46*, 4196−4204.

(23) Mang'era, K. O., Liu, G., Wang, Y., Zhang, Y., Liu, N., Gupta, S., Rusckowski, M., and Hnatowitch, D. J. (2001) Initial investigations of 99mTc-labeled morpholinos for radiopharmaceutical applications. *Eur. J. Nucl. Med. 28*, 1682−1689.

(24) Liu, G., Mang'era, K., Liu, N., Gupta, S., Rusckowski, M., and Hnatowich, D. J. (2002) Tumor pretargeting in mice using 99mTc-labeled morpholino, a DNA analog. *J. Nucl. Med. 43*, 384−391.

(25) Liu, G., Liu, C., Zhang, S., He, J., Liu, N., Gupta, S., Rusckowski, M., and Hnatowich, D. J. (2003) Investigations of technetium-99m morpholino pretargeting in mice. *Nucl. Med. Commun. 24*, 697−705.

(26) He, J., Liu, G., Gupta, S., Zhang, Y., Rusckowski, M., and Hnatowich, D. J. (2004) Amplification targeting: a modified pretargeting approach with potential for signal amplification-proof of a concept. *J. Nucl. Med. 45*, 1087−1095.

(27) He, J., Liu, G., Zhang, S., Vanderheyden, J.-L., Liu, N., Liu, C., Zhang, Y., Gupta, S., Rusckowski, M., and Hnatowich, D. J. (2003) A comparison of in vitro and in vivo stability in mice of two morpholino duplexes differing in chain length. *Bioconjugate Chem. 14*, 1018−1023.

(28) Mistrik, P., Moreau, F., and Allen, J. M. (2004) BiaCore analysis of leptin-leptin receptor interaction: evidence for 1:1 stoichiometry. *Anal. Biochem. 327*, 271−277.

(29) Rossi, E. A., Sharkey, R. M., McBride, W., Karacay, H., Zeng, L., Hansen, H. J., Goldenberg, D. M., and Chang, C. H. (2003) Development of new multivalent-bispecific agents for pretargeting tumor localization and therapy. *Clin. Cancer Res. 9(10 Pt 2)*, 3886s−3896s.

(30) Pack, P., Muller, K., Zahn, R., and Pluckthun, A. (1995) Tetravalent miniantibodies with high avidity assembling in Escherichia coli. *J. Mol. Biol. 246*, 28−34.

(31) Svensson, H. G., Wedemeyer, W. J., Ekstrom, J. L., Callender, D. R., Kortemme, T., Kim, D. E., Sjobring, U., and Baker, D. (2004) Contributions of amino acid side chains to the kinetics and thermodynamics of the bivalent binding of protein L to Ig kappa light chain. *Biochemistry. 43*, 2445−2457.

(32) Muller, K. M., Arndt, K. M., and Pluckthun, A. (1998) Model and simulation of multivalent binding to fixed ligands. *Anal. Biochem. 261*, 149−158.

(33) Kortt, A. A., Lah, M., Oddie, G. W., Gruen, C. L., Burns, J. E., Pearce, L. A., Atwell, J. L., McCoy, A. J., Howlett, G. J., Metzger, D. W., Webster, R. G., and Hudson, P. J. (1997) Single-chain Fv fragments of anti-neuraminidase antibody NC10 containing five- and ten-residue linkers form dimers and with zero-residue linker a trimer. *Protein Eng. 10*, 423−433.

(34) Jenkins, J. L., Lee, M. K., Valaitis, A. P., Curtiss, A., and Dean, D. H. (2000) Bivalent sequential binding model of a Bacillus thuringiensis toxin to gypsy moth aminopeptidase N receptor. *J. Biol. Chem. 275*, 14423−31.

(35) Stenberg, E., Persson, B., Roos, H., and Urbaniczky, C. (1991) Quantitative determination of surface concentration of protein with surface plasmon resonance using radiolabeled proteins *J. Colloid Interface Sci. 143*, 513−526.

BC049719C